DOI: 10.1002/chem.200800300

Squaraines as Reporter Units: Insights into their Photophysics, Protonation, and Metal-Ion Coordination Behaviour

Jose V. Ros-Lis,[a] Ramón Martínez-Máñez,*[a] Félix Sancenón,[a] Juan Soto,[a] Monika Spieles,[b] and Knut Rurack*[b]

Abstract: The synthesis, photophysical properties, protonation, and metal-ion coordination features of a family of nine aniline-based symmetrical squaraine derivatives are reported. The squaraine scaffold displays very attractive photophysical properties for a signalling unit. These dyes show absorption and weakly Stokes-shifted, mirror-image-shaped emission bands in the visible spectral range and there are no hints of multiple emission bands. The mono-exponential fluorescence decay kinetics observed for all the derivatives indicate that only one excited state is involved in the emission. These data stress the interpretation that squaraines can be regarded as polymethine-type dyes. From a coordination chemistry point of view, the squaraines possess four potential binding sites; that is, two nitrogen atoms from the anilino groups and two oxygen atoms from the central C_4O_2 four-membered ring. These coordination sites are part of a cross-conjugated π-system and coordination events with protons or certain metal ions affect the electronic properties of the delocalised π-system dramatically, resulting in a rich modulation of the colour of the squaraines. The absorption band at around 640 nm is blue-shifted when coordination at the anilino nitrogen atoms occurs, whereas coordination to the C_2O_4 oxygen atoms results in the development of red-shifted bands. Addition of more than one equivalent of protons or metal cations could additionally entail mixed *N,O*- or *N,N*-coordinated complexes, manifested in the development of a broad band at 480 nm or complete bleaching in the visible range, respectively. Analysis of the spectrophotometric titration data with HYPERQUAD yielded the macroscopic and microscopic stability constants of the complexes. Theoretical modelling of the various protonated species by molecular mechanics methods and consideration of some of the title dyes within the framework of molecular chemosensing and molecular-scale "logic gates" complement this contribution.

Keywords: dyes/pigments · fluorescence · metal ions · protonation · squaraines

Introduction

In the last 30 years, squaraine dyes[1,2] have attracted strongly increasing attention as deeply coloured and fluorescent units in many optochemical applications, such as optical recording,[3] solar energy conversion,[4] electrophotography,[5] nonlinear optics,[6] photodynamic therapy,[7] biochemical labelling[8] and chromo- and/or fluorogenic probes[9] for various targets such as pH,[10] cations[11] and neutral molecules[12] as well as for the study of self-assembled dye aggregates.[13] The popularity of squaraines is based on their favourable spectroscopic properties. These dyes possess typically narrow and very intense absorption bands (with molar absorption coefficients $\varepsilon > 10^5$) at the red end of the visible spectral window, and rather resonant yet bright fluorescence bands of mirror-image shape with fluorescence quantum yields $\Phi > 0.1$ in polar and aqueous solvents.[14] Attracted by these features, we have also utilised squaraine derivatives in a number of chemical signalling systems for cations,[15,16] anions[17] and neutral molecules.[18,19] Besides functionalisation of the squaraine backbone with suitable receptor units in the classical sense of molecular probes following the "binding site-signalling unit" approach,[20] we especially explored alternative sensing schemes by exploiting the squar-

[a] Dr. J. V. Ros-Lis, Prof. R. Martínez-Máñez, Dr. F. Sancenón, Dr. J. Soto
Instituto de Química Molecular Aplicada
Departamento de Química, Universidad Politécnica de Valencia
Camino de Vera s/n, 46022 Valencia (Spain)
Fax: (+34) 963-877-349
E-mail: rmaez@qim.upv.es.

[b] M. Spieles, Dr. K. Rurack
Div. I.5, Bundesanstalt für Materialforschung und -prüfung (BAM)
Richard-Willstätter-Strasse 11, 12489 Berlin (Germany)
Fax: (+49) 30-8104-5005
E-mail: knut.rurack@bam.de

aines' unique tendency to undergo reversible bleaching reactions upon nucleophilic attack.[16–18]

Apart from the reactivity mentioned in the previous paragraph, squaraines show several other peculiarities, arising from the fact that they can be regarded formally as donor–acceptor–donor-substituted (intramolecular charge-transfer, ICT) chromophores, as doubly cross-linked polymethine-like π-systems or as biradicaloid chromophores (Scheme 1).

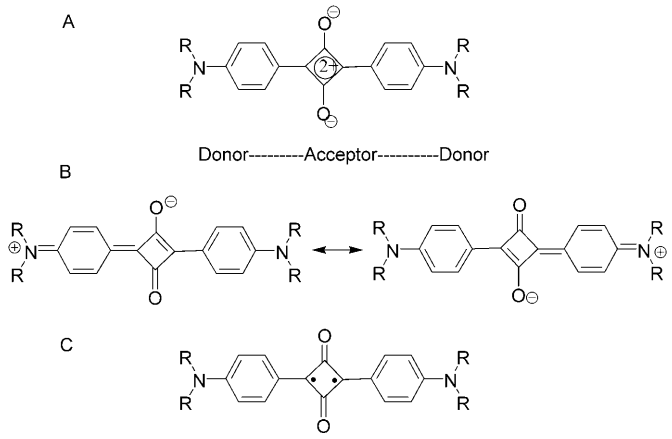

Scheme 1. Possible formal electronic structures of squaraines. In B, only the limiting mesomeric structures are shown, cf. reference [72].

Despite the large number of application-oriented publications (vide infra), squaraines have also received considerable treatment in fundamental studies that make use of NMR spectroscopy,[21] X-ray crystallography,[22] quantum chemical calculations[23] and in various photo-physical studies as a function of solvent nature,[24,25] chemical structure[26] or temperature.[25] However, several contradictory interpretations that have appeared throughout the years in the literature within the context of the use of squaraines as functional dyes or signalling units in molecular probes and other supramolecular ensembles suggest that further insight into the photophysical performance of squaraine reporters is urgently required, especially when the use of such chromophores is extended to areas such as molecular logics,[27,28] multitopic or allosteric and multichannel chemosensors.[29,30] We report here the photophysical properties, and a rationalisation of the colour modulations observed upon interaction with protons and metal cations, of a family of squaraine-based receptors.

Results and Discussion

Synthesis and photophysical properties: Nine representative squaraine dyes were prepared following a general synthetic route, by condensation of aniline derivates with squaric acid in butanol/toluene 1:1 v/v with azeotropic removal of water.[15,18,19,24,31,32] The chemical structures and nomenclature of the prepared compounds are shown here; namely **SNO_3**,[24] **SNO_4**,[24] **SNO_5**,[24] **SNS_2O_2**,[15,19] **SBu**,[31] **SAb**,[18] **SJu**,[32] **SCar**[18] and **SJuOH**.[32] All the derivatives were characterised by standard techniques, including HRMS and NMR spectroscopy. In the latter case, the characteristic doublets in the aromatic region at approximately 6.7 and 8.2 ppm were detected (except for **SJu** and **SJuOH**).

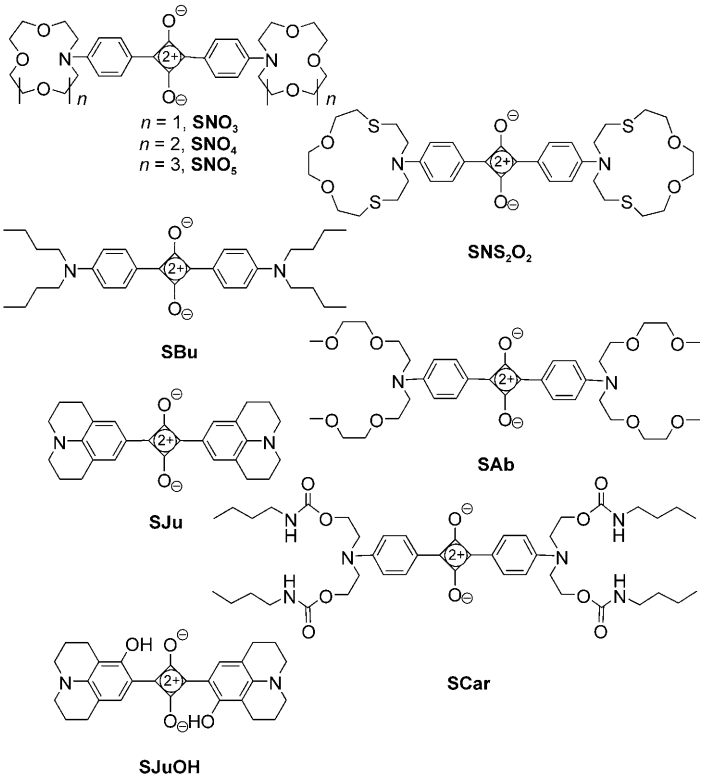

As described in the Introduction, the data in Table 1 and Figure 1 stress the fact that the title dyes show the typical spectroscopic features of squaraines, that is, narrow and intense absorption bands with maxima between 630 and 670 nm, full widths at half maximum (fwhm) of $854 \pm 18\ cm^{-1}$ (except for **SJuOH**: fwhm = $745\ cm^{-1}$), and a weak vibrational shoulder centred at $1434 \pm 30\ cm^{-1}$ (except for **SJuOH** at $1290\ cm^{-1}$) on the high-energy side. The fluores-

Table 1. Photophysical properties of squaraines in MeCN at 298 K.

	λ_{max}^{abs} [nm]	logε [$M^{-1}cm^{-1}$]	λ_{max}^{em} [nm]	Φ_f	τ_f [ns]
SBu	642	5.20	661	0.087	0.46
SNO_3	636	5.16	658	0.078	0.38
SNO_4	634	5.33	654	0.099	0.48
SNO_5	636	5.18	661	0.074	0.43
SNS_2O_2	640	5.49	661	0.129	0.67
SAb	634	5.08	656	0.085	0.47
SCar	629	5.01	651	0.138	0.71
SJu	662	5.29	683	0.041	0.23
SJuOH	666	5.45	681	0.415	2.45

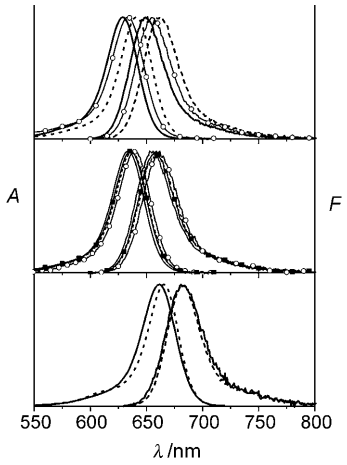

Figure 1. Normalised absorption and fluorescence spectra of the title dyes in acetonitrile at 298 K. Top (from left to right): **SCar** (solid line), **SAb** (symbols), and **SBu** (dotted line); middle (from left to right): **SNO_4** (solid line), **SNO_5** (solid squares), **SNO_3** (dotted line), and **SNS_2O_2** (open circles); bottom: **SJu** (solid line) and **SJuOH** (dotted line).

cence spectra of mirror-image shape are rather resonant, with Stokes shifts between 400 cm^{-1} (for **SJuOH**) and 560 cm^{-1} (for **SNO_3**). The fluorescence excitation spectra match the lowest energy absorption bands in all cases. Fluorescence lifetime measurements yielded monoexponential decay kinetics for all the dyes. These last two findings show that we could not detect any hints for multiple emission bands[26,33] and indicate that only one excited-state species emits. These observations are supported by an analysis of the fluorescence quantum yields and lifetimes by means of the radiative (k_r) and nonradiative (k_{nr}) rate constants according to Equations (1) and (2).

$$k_r = \Phi_f/\tau_f \quad (1)$$

$$k_{nr} = (1-\Phi_f)/\tau_f \quad (2)$$

The values of k_r are very similar for all the compounds investigated here (0.19 ± 0.02 ns^{-1}, see Table 2), and a good linear relationship is obtained between Φ_f and τ_f (Figure 2). From a conformational and transitional point of view, the emissive states of all the dyes are thus very similar. Differences, however, are observed for the nonradiative rate constants. Here, **SJu** shows a particularly high value and **SJuOH** a particularly low value. In the case of **SJuOH**, the deviation is most likely connected to the stabilisation of the chromophore by internal hydrogen bonds between the hydroxyl and carbonyl groups and the reduction of torsional motions around single bonds b1 and b1′, which connect the phenyl rings and the central four-membered ring (Scheme 2). To get better access to the underlying mechanism for the other squaraines, we focused our attention first on the theory of the energy-gap law.[34] According to this rule, the degree of internal conversion is a function of the energy difference between the excited state and the corresponding ground state, as reflected by the emission spectrum/maximum. A reduction in energy gap between these states accelerates internal conversion. If internal conversion is the only major nonradiative process that contributes to quenching, a plot of $\ln k_{nr}$ versus the emission maximum should yield a linear correlation. For the present family of compounds, verification of

Table 2. Additional photophysical parameters of the title compounds.

	k_r [ns^{-1}]	k_{nr} [ns^{-1}]	$\tilde{\nu}_{max}^{em}$ [cm^{-1}]	$\ln k_{nr}$
SBu	0.19	1.98	15082	21.4
SNO_3	0.21	2.43	15159	21.6
SNO_4	0.21	1.88	15243	21.4
SNO_5	0.17	2.15	15174	21.5
SNS_2O_2	0.19	1.30	15095	21.0
SAb	0.18	1.95	15243	21.4
SCar	0.19	1.21	15384	20.9
SJu	0.18	4.17	14619	22.2
SJuOH	0.17	0.24	14619	19.3

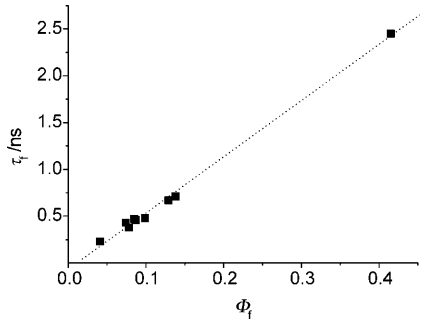

Figure 2. Plot of τ_f versus Φ_f; dotted line exemplifies a linear regression with $r = 0.998$.

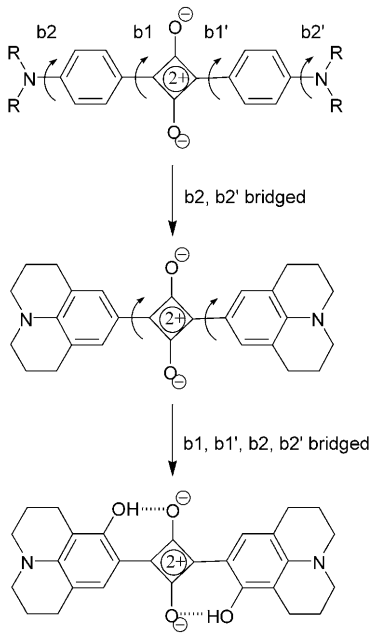

Scheme 2. Flexible bonds in the chromophore and their bridging in **SJu** and **SJuOH**.

such a relationship has to exclude **SJuOH**, based on the reasons given above, and $\mathbf{SNS_2O_2}$, because of the non-negligible contribution of the d orbitals of the sulfur atoms neighbouring the nitrogen atoms. For **SBu**, $\mathbf{SNO_3}$, $\mathbf{SNO_4}$, $\mathbf{SNO_5}$, **SAb**, **SCar**, and **SJu**, a satisfactory linear relationship was indeed found (Figure 3). If we further consider that the dyes obeying the relationship shown in Figure 3 carry partly bulky substituents, which are either very flexible (e.g., **SCar**) or more restricted (e.g., $\mathbf{SNO_3}$), we can conclude that such substituents attached to the aniline nitrogen atoms have a negligible influence on torsional motions around bonds b1 and b1′. Only direct fixation of these bonds by internal hydrogen bonding as in **SJuOH** evidently makes a difference (Scheme 2). Furthermore, the negligible influence of the size and topology of the substituents at the aniline groups, and the fact that **SJu**, for which the aniline groups are fixed in a planar conformation, also fits well into the energy-gap correlation suggest that torsional motions around bonds b2 and b2′ also play only a very minor role in excited state deactivation (Scheme 2).

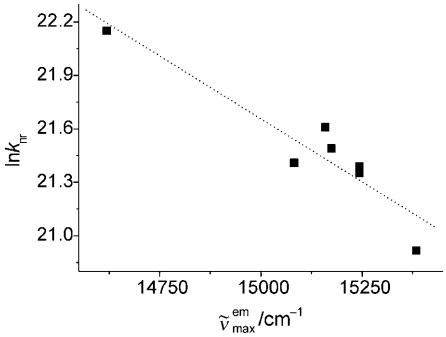

Figure 3. Plot of $\ln k_{nr}$ versus $\tilde{\nu}^{em}_{max}$; data set excludes points for $\mathbf{SNS_2O_2}$ and **SJuOH** (see text), dotted line exemplifies a linear regression with $r = 0.935$.

To get a better insight into the chromophoric nature of the title dyes, **SBu** and a series of model compounds **M1**–**M5** (Figure 4) were treated theoretically by using density functional theory (DFT) with the B3LYP functional and the 6-31G basis set as implemented in Gaussian 03. The main question is whether squaraines such as **SBu** more closely resemble cyanine dyes or donor–acceptor(–donor)-substituted stilbene, coumarin or styryl dyes, which are commonly referred to as "D–A(–D) dyes" in the literature,[35,36] because they show all the features of ICT dyes.[37] When invoking an analysis of the frontier molecular orbitals (MOs) of the geometry-optimised ground-state structures, two features are important. According to the triad theory of organic dyes, the first key feature of a polymethinic character is an alternating π electron density, that is, HOMO and LUMO should show an increasing tendency for alternation upon approximating the ideal polymethine state.[38] Figure 4 reveals that both of the simplest models studied here, **M1** and **M2**, largely fulfil this requirement (see also discussion in reference [39]). The second important feature relates to the symmetry and delocalisation of the MOs.[40] Here, the situation is distinctly different for **M1** and **M2**. Whereas both HOMO and LUMO are symmetric and delocalised over the entire π system in cyanine **M1**, they are largely localised on the respective donor (dimethylaniline) and acceptor (methylpyridinium) fragments for a classic D–A dye such as **M2**. Consequently, **M1** displays narrow and structured absorption and emission bands and a negligible solvatochromism.[41] In contrast, **M2** shows considerably broader absorption and emission bands (especially in polar solvents) and a pronounced solvatochromism due to an ICT process involving donor and acceptor moieties.[42] Comparison of **SBu** with a true squarylium cyanine (**M3**)[43] and other symmetric D–A–D dyes (**M4**, **M5**)[44,45] indicates that **SBu** more closely resembles cyanine dyes such as **M1** and **M3** than ICT or D–A(–D) dyes such as **M2**, **M4**, and **M5**, the last two also showing similar spectroscopic features to **M2**, that is, broad, solvatochromic bands.

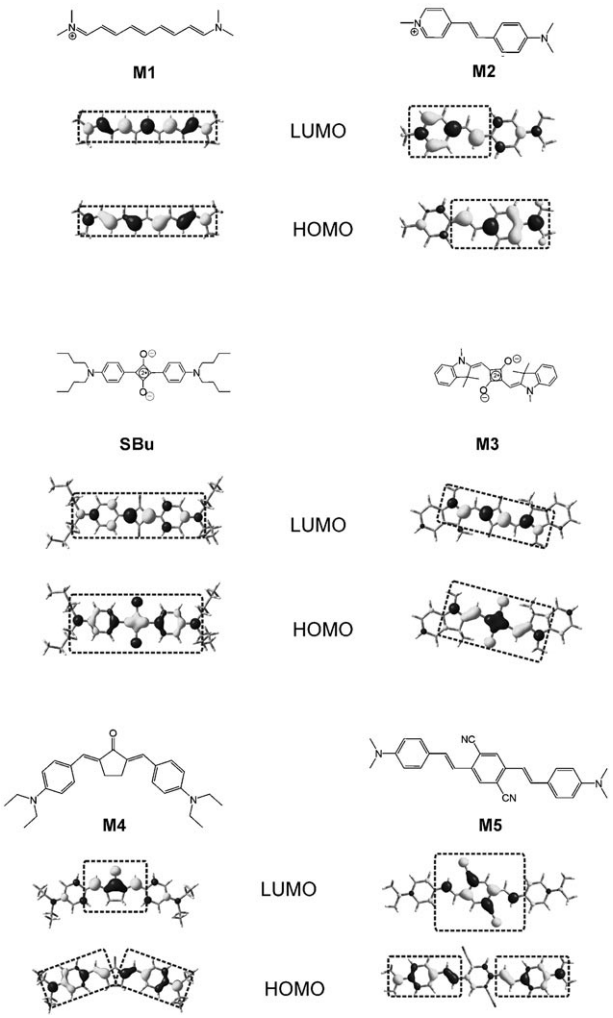

Figure 4. Frontier MOs of **SBu** and model compounds **M1**–**M5** as obtained from the DFT quantum chemical calculations; dashed boxes indicate main region of MO localisation. Similar features of MO localisation as observed here for **SBu** have also been found for other squaraines with more elaborate endgroups, see for example references [73,74].

Our present experimental and theoretical results, in combination with the lack of a pronounced solvatochromism as found by Cornelissen-Gude et al.[25] and the negligible influence of intersystem crossing,[46] suggest that the states of the squaraines involved in the optical transitions have a more polymethinic than intramolecular charge-transfer (ICT) character, often associated with donor–acceptor(–donor)-substituted dyes. In contrast, the moderate fluorescence quantum yields in acetonitrile observed for all the dyes except **SJuOH** and the strong "positive solvatokinetic behaviour" (a decrease in emission yield with increasing solvent polarity) reported for such compounds previously[25] indicate that an intramolecular charge separation process in the excited state, involving large amplitude motions around b1 and b1′, is nonetheless important. However, this process does not produce another emissive species, but leads to the population of an entirely non-emissive species, most likely connected to the concept of twisted intramolecular charge-transfer (TICT) states.[47] Support is also furnished by investigations of solute–solvent complexes[21] or squaraines that are pretwisted, because of the introduction of bulky substituents in *ortho* position to the b1,b1′ bonds,[26] both of which revealed decreased fluorescence quantum yields.

Spectroscopic studies involving protons: From the point of view of chemical addressability, the popularity of squaraines as reporter molecules is mainly based on the fact that they possess four potential sites of interaction with chemical species: two nitrogen atoms from the aniline groups and two oxygen atoms from the central C_4O_2 ring. These sites are part of the same conjugated π system, and interaction with, for instance, protons or metal ions will dramatically affect the electronic properties of the chromophore. As a consequence, colour modulations are to be expected (vide infra). As a first step to assess the influence of the different substituents at the aniline on these spectroscopic responses, the protonation behaviours of **SNS_2O_2**, **SBu**, **SJu**, **SJuOH**, **SNO_3**, and **SCar** were studied in acetonitrile.

The first effect that we will discuss is a hypsochromic shift of the squaraine absorption band upon addition of one equivalent of acid, resulting in a colour change from blue to violet. The titration spectra in Figure 5 show one example: the appearance of a new absorption band at around 560 nm with a well-defined isosbestic point for **SNO_3** in the presence of up to one equivalent of protons. In accordance with the shift observed upon exchange of one of the dimethylamino groups by a methoxy group, that is, exchange of a strong donor in **SDMA** with $\lambda_{max}^{abs} = 627$ nm in chloroform for a weaker donor in **USNO**, absorbing at 579 nm;[48,49] we attribute this shift to exclusive protonation of one nitrogen atom. It is known that the small macrocycle in **SNO_3** stabilises protonation of the nitrogen atom by hydrogen bonding interactions in nonprotic solvents.[24,50] At higher acid concentrations, gradual bleaching of the solution occurs because of the disappearance of the band at approximately 560 nm (Figure 5). These changes are attributed to the step from **SNO_3H^+** to **$SNO_3H_2^{2+}$**, switching off also the second polymethinic branch. This interpretation is supported by the fact that deeply coloured, positively charged, hemicyanine dyes that carry an amino crown ether group as one terminal unit undergo strong decolouration upon cation binding.[51] Similar colour changes upon protonation of the aniline moieties are found for **SJuOH** for equimolar amounts of acid ($\lambda_{max}^{abs} =$ 526 nm). In this case, the existence of intramolecular hydrogen bonds between the OH groups and the oxygen atoms from the C_4O_2 central ring decreases the basicity of the oxygen atoms, favouring protonation at the aniline, but only one protonation step is observed in the acid concentration range studied (0.1 μM $< c_{H^+} <$ 1 mM).

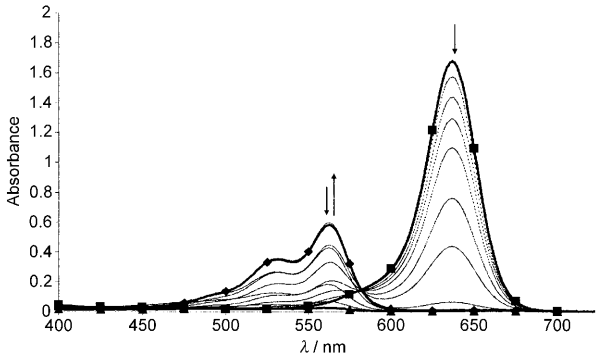

Figure 5. Spectroscopic behaviour of **SNO_3** in acetonitrile as a function of increasing proton concentration. ■ = initial spectrum, ◆ = spectrum at equimolar ratios of H^+ and **SNO_3** and ▲ = endpoint spectrum; dashed lines = intermediate titration spectra.

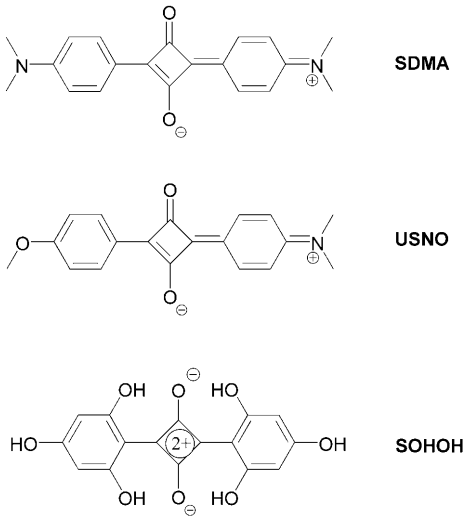

Features opposite to those found for **SNO_3** are recognised when **SJu** is titrated with up to equimolar amounts of acid. Again, the typical squaraine band centred at 660 nm disappears. However, for **SJu** a bathochromically shifted absorption band develops at about 690 nm, with well-defined isosbestic points again indicating a straightforward equilibrium **SJu** $+ H^+ \rightleftarrows$ **SJu**H^+ (Figure 6). This bathochromic shift is attributed to the protonation of an oxygen atom of the central ring. The change in protonation preference is probably connected to the steric fixation of the aniline's nitrogen atom in

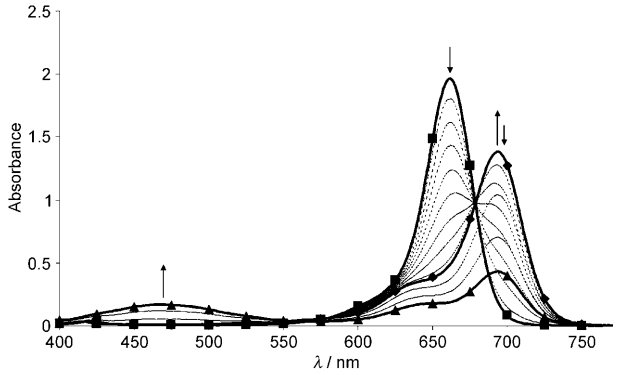

Figure 6. Spectroscopic behaviour of **SJu** in acetonitrile as a function of increasing proton concentration. ■ = initial spectrum, ◆ = spectrum at equimolar ratios of H^+ and **SJu** and ▲ = endpoint spectrum; dashed lines = intermediate titration spectra.

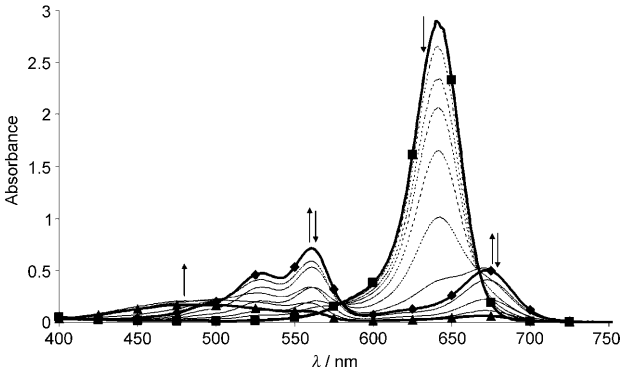

Figure 7. Spectroscopic behaviour of **SBu** in acetonitrile as a function of increasing proton concentration. ■ = initial spectrum, ◆ = spectrum at equimolar ratios of H^+ and **SBu** and ▲ = endpoint spectrum; dashed lines = intermediate titration spectra.

the julolidine group, which acts as a counterforce for the transition of a planar (quasi-sp^2) aniline nitrogen into a tetrahedral (quasi-sp^3) anilinium nitrogen. Additionally, the nitrogen atoms' lone electron pairs are better delocalised in the entire julolidine moiety than in an alkylaniline group. The latter also leads to an increase of the electron density at the central oxygen atoms. At equimolar ratios, one oxygen atom is thus protonated. With a higher excess of acid, bleaching of the band at around 690 nm occurs and a new band is formed at 470 nm. The latter is very broad and considerably weaker in intensity. Such changes correspond to a loss of the cyanine nature of the chromophore and suggest that the doubly protonated species possesses a certain charge-transfer character, hence the second protonation step occurs at a nitrogen atom. Interestingly, **SCar** shows a very similar behaviour, that is, a bathochromic shift up to equimolar ratios of acid. However, because the neighbouring carbamate groups distinctly reduce the tendency for aniline protonation, a second protonation step could not be achieved here in the acid concentration range studied (0.1 μM < c_{H^+} < 1.2 mM).

A third type of response is registered for **SNS_2O_2** and **SBu**. Addition of up to one equivalent of acid results in the simultaneous development of blue- and red-shifted bands, indicating rather similar basicities of N and O atoms and statistical protonation at both sites. Furthermore, addition of an excess of acid to **SNS_2O_2** as well as **SBu** induces the development of a new band at 470 nm, suggesting the formation of species protonated at one nitrogen and one oxygen atom (Figure 7).

Unfortunately, none of the protonated species showed a measurable fluorescence, so it was not possible to obtain additional information by employing this technique. However, such a loss of fluorescence is in agreement with the fact that already neutral but asymmetric dyes such as **USNO** show strongly quenched emission ($\Phi_f < 10^{-3}$ already in a medium polar solvent such as $CHCl_3$).[48] Moreover, in their protonation studies of **SOHOH**, Das et al. found that only the neutral derivative is fluorescent.[52] In the protonated species, excited-state charge shift/rearrangement reactions leading to fast nonradiative decay through conical intersections seem to be responsible for efficient quenching.[53] Table 3 summarises the observed relationship between the changes in absorption and the site of protonation.

Table 3. Colour modulation and protonation sites.

Protonated atom	λ_{max} [nm] approx.
none protonated	640
N	560
O	670
N and O	470
N and N	no band

The extent of the colorimetric shift in the squaraine family is evidently related to protonation at different sites and a delicate balance between the basicity of the nitrogen and oxygen atoms in the chromophore. A detailed analysis of the spectrophotometric titration data has thus been carried out with the HYPERQUAD program (see Experimental Section). Macroscopic protonation constants $\log K_n$ were calculated for the representative compounds **SNS_2O_2**, **SBu**, **SJu**, **SJuOH** and **SNO_3** and are shown in Table 4. As stated above, **SJuOH** is only protonated at the oxygen, whereas **SJu**, **SNO_3**, **SNS_2O_2** and **SBu** are protonated twice. Moreover, for **SJu** and **SNO_3** the two protonation steps are well separated and it is possible to determine the stability constants $\log K_{1,2}$ for individual protonation at the nitrogen and oxygen atoms. In contrast, in the case of **SNS_2O_2** and **SBu**,

Table 4. Logarithm of the macroscopic (K) and overall (β) protonation constants for selected squaraine derivatives in acetonitrile (298 K); $\log\beta = \Sigma\log K_n$.

Reaction		**SNS_2O_2**	**SBu**	**SJu**	**SJuOH**	**SNO_3**
$[L]+H^+ \rightleftarrows [LH]^+$	$\log K_1$	5.42(9)	5.9(1)	5.3(1)	5.9(6)	6.3(7)
$[LH]^+ + H^+ \rightleftarrows [LH_2]^{2+}$	$\log K_2$	3.1	2.9	2.9	–	4.7
$[L]+2H^+ \rightleftarrows [LH_2]^{2+}$	$\log\beta$	8.52(2)	8.8(0)	8.15(0)	–	11.1(1)

the complex spectral changes shown in Figure 7 indicate that the two protonation steps at the nitrogen and oxygen atoms are not well separated, leading to macroscopic/apparent $\log K_1$ values of 5.42 and 5.9, respectively, characterizing the basicity of the molecules as a whole. These macroscopic constants, however, fail to provide information on the specific proton-binding sites. Nevertheless, site-specific basicities can be obtained by determination of the microscopic constants, $\log k_{N/O}$. These data are shown in Table 5. In combination with the data of Table 4 it is evident that protonation at the oxygen atoms requires similar acidities ($\log k_O \approx 5.3$ for **SNS_2O_2** and **SBu** as well as $\log K = \log k_O = 5.3$ for **SJu**), whereas protonation at the nitrogen atoms varies for all of the dyes. This observation is in agreement with the variety of different substitution patterns at the aniline group, ranging form $\log K = \log k_N = 6.3$ for **SNO_3** (stabilisation by internal hydrogen bonds, see above) to $\log k_N = 4.61$ for **SNS_2O_2** (aggravated protonation due to neighbouring sulfur atoms).

Table 5. Logarithm of the macroscopic (K) and microscopic (k) protonation constants of **SNS_2O_2** and **SBu** in acetonitrile (298 K).

Reaction	$\log K$	$\log k_N$	$\log k_O$	$\log k_{N,O}$	$\log k_{O,N}$
$[SNS_2O_2]+H^+ \rightleftarrows [SNS_2O_2H]^+$	5.42(9)	4.61	5.34	3.91	3.18
$[SBu]+H^+ \rightleftarrows [SBuH]^+$	5.9(1)	5.74	5.37	3.06	3.43

If we look to the second protonation step ($\log K_2$), the values are two to three orders of magnitude lower than the first protonation constants, in agreement with the additional electrical work necessary to protonate species that are already positively charged. Additionally, a detailed look at the squaraine derivatives able to be protonated twice allows the identification of two different behaviours. Whereas **SNS_2O_2**, **SBu** and **SJu** finally yield N,O-protonated species with $\log K_2 \approx 3$ for the $HL^+ + H^+ \rightleftarrows H_2L^{2+}$ process, the $HL^+ + H^+ \rightleftarrows H_2L^{2+}$ process of **SNO_3** with $\log K_2 = 4.7$ produces an N,N-protonated species. This difference in the second protonation constant can be explained by electrostatic repulsion, which should be larger for the conjugated N,O-protonation sites than for the cross-conjugated N,N-protonation sites.

As additional support, the relative hydrogen-bond donating and accepting abilities (i.e., basicities) of the N and O atoms were derived in a comparatively simple way from the protonation energies in the gas phase at particular molecular sites of the PM3-optimised ground state geometries of **SBu**, **SNO_3** and **SJu**. The proton affinities were calculated by subtracting the energy of the neutral form from the energy of the various protonated species, $\Delta E_H = E(sqH_n^{n+}) - E(sq)$. **SBu**, **$SNO_3$** and **SJu** were taken as representative examples because they display a clearly different behaviour upon protonation (see above). The calculated results are shown in Table 6. Here, the lower the value of ΔE_H the higher the ability of the protonation site to accept hydrogen bonds, that is, the more basic is the site. Table 6 reveals that the theoretical results are in agreement with the spectroscopic behaviour. Whereas N-protonation is favoured in **SBu** and **SNO_3**, protonation at an oxygen atom is preferred in **SJu**. The calculations for the second protonation step suggest that in the case of **SBu** and **SJu** the complementary atom is favoured, leading to N^+H,OH species in accordance with the experiments. In addition, the results on **SNO_3** in Table 6 support N,N-protonation. The third protonation then is energetically highly unfavourable and could also not be achieved experimentally for the squaraines studied.

Table 6. Proton affinities for **SBu**, **SJu** and **SNO_3** calculated using the PM3 semiempirical molecular model through subtraction of the energy of the deprotonated [E(sq)] form to the energy of the protonated molecule [$E(sqH_n)$].

Number of protons (n)	Protonated atoms	$E(sqH_n)-E(sq)$ [Kcal mol^{-1}]		
		SBu	**SJu**	**SNO_3**
0	–	0	0	0
1	O	74.6	77.1	93.8
	N	60.3	88.8	90.6
2	O-O	248.0	248.9	243.1
	N-N	221.6	247.7	209.6
	N-O	194.1	219.1	214.3
3	N-O-O	424.1	446.4	437.4
	N-N-O	428.1	452.1	443.9

Spectroscopic studies involving metal ions: The protonation experiments provided a first valuable insight into the different basicities of the squaraines' heteroatoms as a function of substituents. To elucidate the additional effect of coordinative forces on the signalling expression of squaraines, we next investigated the title compounds' response in the presence of various metal ions in acetonitrile. Again, spectroscopically similar changes as described above can occur, that is, a blue shift of the band at around 640 nm for cation coordination to the anilino nitrogen or a red-shifted band upon coordination to the C_2O_4 oxygen atoms. If, additionally, a second metal ion is bound, either mixed N,O- or N,N-coordinative complexes can be formed, resulting in the development of a broad band at 480 nm or bleaching. The colorimetric behaviour of the ligands in the presence of one equivalent or an excess of certain metal cations is summarised in Table 7. Also, for selected systems the stability constants for the formation of complexes have been determined and are shown in Table 8.

Among the alkali (Li^+, Na^+, K^+) and alkaline earth metal (Mg^{2+}, Ca^{2+}, Ba^{2+}) cations tested, only Ba^{2+} was able to induce changes, and only with the **SNO_5** derivative. A hypsochromic shift of 50 nm with a change of colour from blue to purple was observed upon addition of one equivalent of Ba^{2+} (Figure 8a). This behaviour agrees with an interaction of the metal ion through the macrocycle and is in accordance with the ability of N-substituted A18C6 to bind Ba^{2+}.[54] Addition of an excess of Ba^{2+} resulted in no further change, indicating that **SNO_5** is only able to bind one cation. Apparently, the binding constant for A18C6-Ba^{2+} ($\log K = 4.55$) is too small to overcome the electrostatic repulsion for a positively charged complex to bind another twofold posi-

Table 7. Summarised UV/vis absorption behaviour of the squaraine derivatives upon addition of Ba^{2+}, Hg^{2+}, Fe^{3+}, Pb^{2+}, Cu^{2+} and H^+.

	Ba^{2+}		Hg^{2+}		Fe^{3+}		Pb^{2+}		Cu^{2+}		H^+	
	1 equiv	excess	1 equiv	excess	1 equiv	excess	1 equiv	excess	1 equiv	excess	1 equiv	excess
SNS_2O_2	–	–	560	bleaching	670	670	–	–	560	No	560/670	480
SBu	–	–	670	670	670/560	670/560	–	–	670	480	560/670	480
SAb	–	–	560/670	560/670	670/560	670/560	–	–	670	480	–	–
SJu	–	–	560	560	560	500	–	–	560	500	670	480
SJuOH	–	–	560	560	560	500	–	–	560	500	560	560
SNO_3	–	–	560/670	560/670	670/560	670/560	560	560	670	480	560	bleaching
SNO_4	–	–	560/670	560/670	670/560	670/560	560	560	670	480	–	–
SNO_5	560	560	560	560	670/560	670/560	560	bleaching	670	480	–	–
SCar	–	–	670	670	670	670	–	–	670	480	670	670

Table 8. Logarithm of the stability constants for the interaction of the squaraine derivatives with Ba^{2+}, Pb^{2+}, Hg^{2+} and Cu^{2+} in acetonitrile (298 K).

Reaction		**SNS_2O_2**	**SBu**	**SAb**	**SJu**	**SJuOH**	**SNO_3**	**SNO_4**	**SNO_5**
$[L]+Ba^{2+}\rightleftarrows[LBa]^{2+}$		–	–	–	–	–	–	–	4.55(1)
$[L]+Pb^{2+}\rightleftarrows[LPb]^{2+}$	$\log K_1$	–	–	–	–	–	3.69(3)	4.54(9)	7.9(7)
$[LPb]^{2+}+Pb^{2+}\rightleftarrows[LPb_2]^{4+}$	$\log K_2$	–	–	–	–	–	–	–	4.0
$[L]+2Pb^{2+}\rightleftarrows[LPb_2]^{4+}$	Logβ	–	–	–	–	–	–	–	11.9(3)
$[L]+Hg^{2+}\rightleftarrows[LHg]^{2+}$	$\log K_1$	9.2(3)	4.45(5)	4.29(5)	5.3(6)	4.93(8)	4.91(8)	4.49(7)	4.80(2)
$[LHg]^{2+}+Hg^{2+}\rightleftarrows[LHg_2]^{4+}$	$\log K_2$	6.7	–	–	–	–	–	–	–
$[L]+2Hg^{2+}\rightleftarrows[LHg_2]^{4+}$	Logβ	15.9(6)	–	–	–	–	–	–	–
$[L]+Cu^{2+}\rightleftarrows[LCu]^{2+}$	$\log K_1$	7.0(3)	6.6(0)	6.3(8)	6.1(5)	6.8(1)	6.5(2)	6.6(2)	6.44(7)
$[LCu]^{2+}+2Cu^{2+}\rightleftarrows[LCu_2]^{4+}$	$\log K_2$	3.1	5.6	6.0	5.6	4.9	5.8	5.1	5.5
$[L]+2Cu^{2+}\rightleftarrows[LCu_2]^{4+}$	Logβ	10.1(3)	12.1(8)	12.4(3)	11.7(4)	11.7(0)	12.3(0)	11.7(5)	11.98(6)

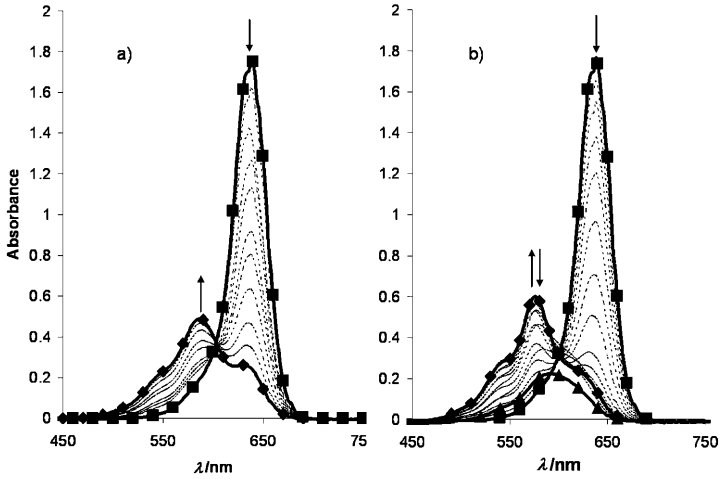

Figure 8. Spectroscopic behaviour of **SNO_5** in acetonitrile upon increasing amounts of a) Ba^{2+}, b) Pb^{2+}. a) ■ = initial spectrum, ◆ = endpoint spectrum, dashed lines = intermediate titration spectra. b) ■ = initial spectrum, ◆ = spectrum at equimolar ratios of Pb^{2+} and **SNO_5**, ▲ = endpoint spectrum, dashed lines = intermediate titration spectra.

tively charged species. Pb^{2+} also induces changes for **SNO_5** (Figure 8b), and to a minor extent with **SNO_4** and **SNO_3**. This result is in agreement with the larger radius of Pb^{2+}, which apparently fits well into the larger cavity of the **SNO_5** receptor. Figure 8b shows that the spectra of **SNO_5**–Ba^{2+} and **SNO_5**–Pb^{2+} are similar, with the development of a band at 576 nm. However, in the case of Pb^{2+} and **SNO_5**, the presence of more than one equivalent of metal ion leads to the disappearance of the absorption band. The latter can be attributed to a stronger $Pb^{2+}\cdots$N interaction with a more covalent character, which results in a more efficient capture of the electron pair of the nitrogen.[55] These favourable binding features are reflected in the stability constant obtained for the formation of the $[$**SNO_5**$Pb]^{2+}$ complex ($\log K = 7.9$), which is almost two orders of magnitude larger than that for the formation of $[$**SNO_5**$Ba]^{2+}$ (see Table 8). Moreover, this strong interaction of Pb^{2+} with **SNO_5** allows a second cation to be bound in the second crown with $\log K = 4.0$ for the process $[LPb]^{2+}+Pb^{2+}\rightleftarrows[LPb_2]^{4+}$, see Table 8.

Addition of Cu^{2+}, Fe^{3+} and Hg^{2+} induced colour changes for all the squaraine dyes, with Hg^{2+} exhibiting the most interesting behaviour. In the case of **SBu**, the butyl chains do not favour, in general, the interaction of the anilino nitrogen atoms with cations and the presence of Hg^{2+} leads to the evolution of a red-shifted band at 656 nm that is assigned to coordination of Hg^{2+} with one oxygen atom of C_4O_2. Similar coordinative behaviour has been found for **SCar**. Moving to receptors with better aniline ligating units we also start to observe a band at 560 nm, indicative of partial coordination at the aniline. This band is not very important for **SAb** (Figure 9a), but significant for **SNO_4** (Figure 9b), indicating mixed nitrogen and oxygen coordination. Accordingly, **SNS_2O_2** only forms species in which Hg^{2+} is bound at the macrocycle, as indicated by the development of the hypsochromically shifted band at 582 nm (upon addition of up to one equivalent of Hg^{2+}, Figure 9c). In this case, addition of more than one equivalent of Hg^{2+} resulted in a bleaching of the solution, suggesting the formation of species where two Hg^{2+} ions occupy both macrocycles. The stability constants calculated for the formation of the Hg^{2+} complexes with **SNS_2O_2**, **SBu**, **SAb**, **SJu**, **SJuOH**, **SNO_3**, **SNO_4** and **SNO_5** are

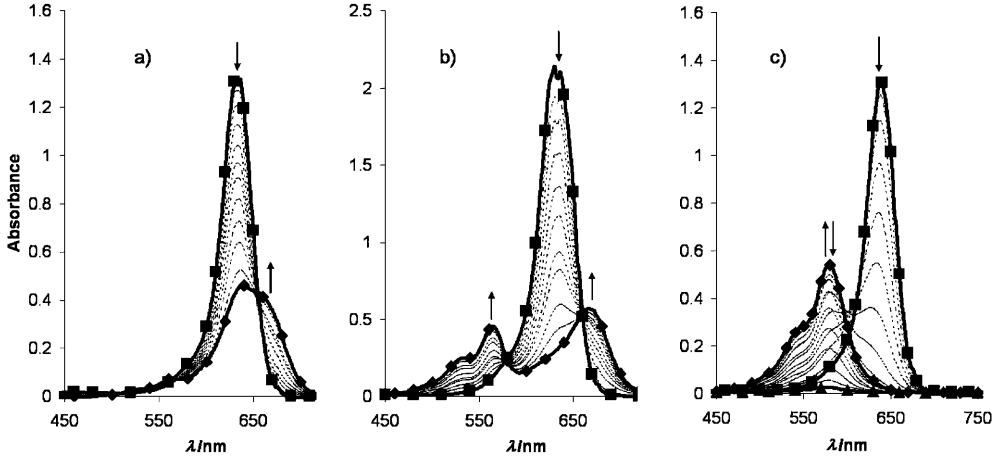

Figure 9. Spectroscopic behaviour in acetonitrile upon increasing amounts of Hg^{2+} for a) **SAb**, b) **SNO_4** and c) **SNS_2O_2**. a) and b) ■ = initial spectrum, ◆ = endpoint spectrum, dashed lines = intermediate titration spectra. c) ■ = initial spectrum, ◆ = spectrum at equimolar ratios of Hg^{2+} and **SNS_2O_2**, ▲ = endpoint spectrum, dashed lines = intermediate titration spectra.

shown in Table 8. All these squaraine derivatives except **SNS_2O_2** form 1:1 metal-to-ligand complexes. For **SNS_2O_2**, the $[LHg_2]^{4+}$ species is also found. Moreover, whereas **SJu**, **SJuOH** and **SNO_5** display nitrogen coordination, **SBu** and **SCar** show oxygen coordination with the Hg^{2+} cation. Additionally, for the ligands **SAb**, **SNO_3** and **SNO_4** for which mixed N,O-coordination was found, the microscopic constants for Hg–O and Hg–N coordination have also been calculated (Table 9). As expected, derivation of the macroscopic and microscopic binding constants yields comparable oxygen coordination constants ($4.27 < \log K < 4.45$). These values are rather large for oxygen–Hg^{2+} coordination when one considers that no macrocycle or chelating arm is present to stabilise the complex, but agree with the existence of a partial negative charge at the oxygen. On the contrary, the nitrogen–Hg^{2+} binding constants show higher scattering ($2.82 < \log K < 9.2$). The largest $\log K = 9.2$ for N–Hg^{2+} binding is found for the formation of $[(\mathbf{SNS_2O_2})Hg]^{2+}$, indicating a very strong interaction of the sulfur-containing macrocycle with the mercuric cation. A recently reported system containing the same aza–thia–oxa macrocycle appended to a phenoxazinone dye showed $\log K = 6.07$ for the formation of the Hg^{2+} complex in water.[56] Furthermore, the strong interaction of Hg^{2+} with the aza–thia–oxa macrocycle prevents metal coordination at the central C_4O_2 group and produces the 1:2 complex $[(\mathbf{SNS_2O_2})Hg_2]^{4+}$ with both macrocycles coordinated ($\log K = 6.7$ for $[LHg]^{2+} + Hg^{2+} \rightleftarrows [LHg_2]^{4+}$). Again, the second binding constant is lower than the first due to electrostatic repulsion, but is still larger than those found for O–Hg^{2+} coordination.

Table 9. Logarithm of the macroscopic (K) and microscopic (k) stability constants for the interaction of the squaraine derivatives **SAb**, **SNO_3** and **SNO_4** with Hg^{2+} in acetonitrile (298 K).

Reaction	$\log K$	$\log k_N$	$\log k_O$
$[\mathbf{SAb}] + Hg^{2+} \rightleftarrows [\mathbf{SAb}Hg]^{2+}$	4.29(5)	2.82	4.27
$[\mathbf{SNO_3}] + Hg^{2+} \rightleftarrows [\mathbf{SNO_3}Hg]^{2+}$	4.91(8)	4.78	4.32
$[\mathbf{SNO_4}] + Hg^{2+} \rightleftarrows [\mathbf{SNO_4}Hg]^{2+}$	4.49(7)	3.96	4.35

Cu^{2+} shows a much more homogeneous behaviour than Hg^{2+}. This is exemplified in Figure 10, which shows the colour modulations in the **SBu**–Cu^{2+} system. Similar graphs and $\log K$ were obtained for **SAb**, **SNO_3**, **SNO_4**, **SNO_5** and **SCar** (see Table 8). At low metal-to-dye ratios a band develops at 660 nm and is assigned to the interaction of Cu^{2+} with a central oxygen atom from the C_4O_2 group. Further addition of Cu^{2+} results in the elimination of this band and the appearance of a new, broad absorption band at about 430 nm, indicating the formation of a bimetallic complex with Cu^{2+} ions coordinating at one oxygen and one nitrogen atom. In contrast to this general behaviour, interaction of **SNS_2O_2** with Cu^{2+} results in a hypsochromic shift (band at

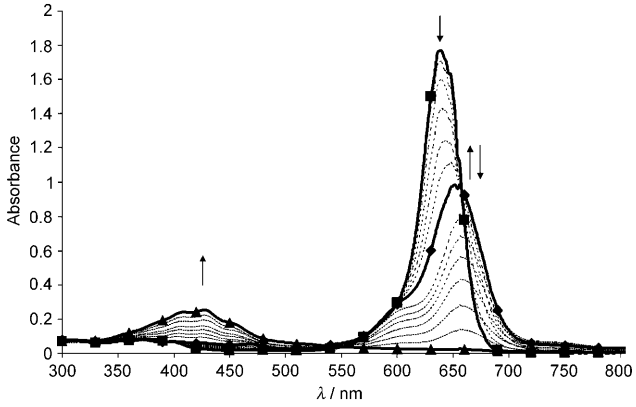

Figure 10. Spectroscopic behaviour of **SBu** in acetonitrile upon increasing amounts of Cu^{2+}. ■ = initial spectrum, ◆ = spectrum at equimolar ratios of Cu^{2+} and **SBu**, ▲ = endpoint spectrum, dashed lines = intermediate titration spectra.

624 nm) because of metal coordination through the macrocycle. This shift with Cu^{2+} is remarkably lower than with Hg^{2+} ($\lambda_{max}=582$ nm), suggesting weaker interaction of Cu^{2+} with the nitrogen bridge head atom. Additionally, the presence of an excess of Cu^{2+} induces an elimination of the band due to the simultaneous Cu^{2+} coordination by both macrocycles of $\mathbf{SNS_2O_2}$.

Finally, Fe^{3+} also shows a diverse and rather complex behaviour that is summarised in Table 7.

Signalling paradigms: Squaraines are very attractive and popular scaffoldings for chemically addressable colour modulations. As shown above, chemical inputs such as protons or metal ions are readily transformed into dramatic spectroscopic changes, creating various output patterns. Such versatile chemical input–optical output features are of timely significance and have been widely applied in two closely related fields: molecular chemosensing and molecular-scale "logic gates". In the former, optical signals are used to detect the presence of certain chemical species in solution.[37,57] In the second approach, chemical species are treated as inputs that control, through Boolean logic rules, the output, which is usually a light signal.[27,58] In the chemosensing field, the goal is often selectivity, that is, a unique chemical species should induce a unique change in colour or fluorescence. In contrast, molecular logic looks for more complex systems, which usually contain multiple binding sites and show certain unique response patterns, exemplifying the desired logic operation, in the presence of either or both inputs (three-input systems are of course even more complex).

With respect to squaraines, the results for our title compounds presented here suggest that those dye/input combinations that give diverse photometric responses might be suitable for the design of molecular logic devices, while selective binding of a guest with only a specific group on the dye can result in selective chromo-fluorogenic chemosensors. In the following, we will review the above given results in view of these two concepts.

Molecular-scale logic gates: The cation-induced modulations of the squaraines' absorption spectrum involve the appearance or disappearance of various bands located at about 640, 560, 670, and 480 nm as well as complete bleaching in the visible region, and can be divided into four cases: single N-, single O-, N,O- and exclusive N,N-coordination. Thus, coordination at different sites could open different channels related to the absorption properties of the final ensemble. This is a rich behaviour that could be of interest in the development of molecules with intrinsic logic capability. Molecular logics is an interesting concept and many examples have been developed since it was noticed that the interaction of a receptor molecule with certain species (input) can yield response (output) patterns that follow Boolean logic rules.[27,58] Tables 10 and 11 summarise some general response patterns. For instance, Table 10 shows how the absorption response of the $\mathbf{SNS_2O_2}/Hg^{2+}$ system obeys NOR, AND, and XOR logics.[59] Additionally, Table 11 shows the optical response for the system **SJu** (processor), H^+ (input A), and Hg^{2+} (input B), which results in NOR, ID-A, and ID-B Boolean algebraic functions. Some other different logics can be designed bearing in mind the response of the different ligands in the presence of protons or metal cations at different concentrations (Table 7 summarises this behaviour) and the corresponding stability constants. The title dyes thus belong to the class of multifunctional dyes that contain two or more sites for an interaction with chemical species and that respond to more than a single input. Such molecules are commonly referred to as "reconfigurable" molecular logic gates, that is, as systems in which it is possible to observe different logic expressions from one unique molecular entity.[60]

Table 10. 2-Inputs logic truth tables for colour modulations of $\mathbf{SNS_2O_2}$ with Hg^{2+} concentrations as input.

Input A Hg^+ (1 equiv)	Input B Hg^{2+} (1 equiv)	Output 1 640 nm band	Output 2 560 nm band	Output 3 Bleaching
0	0	1	0	0
1	0	0	1	0
0	1	0	1	0
1	1	0	0	1

Table 11. 2-Inputs logic truth tables for **SJu** with H^+ and Hg^{2+} as inputs.

Input A H^+(1 equiv)	Input B Hg^{2+}(1 equiv)	Output 1 640 nm band	Output 2 560 nm band	Output 3 670 nm band
0	0	1	0	0
1	0	0	0	1
0	1	0	1	0
1	1	0	1	1

Molecular chemosensing: From the point of view of chemosensing, the behaviour of most of the title compounds is far from being suitable, because of the considerably low selectivity observed. However, this is relatively common when using a poorly coordinating solvent such as acetonitrile. In acetonitrile, there is no serious competition by the solvent and many metal ions can often interact even with nonsupported coordination sites, such as the oxygen atoms of the central ring in our case. When moving from acetonitrile to acetonitrile–water mixtures or to neat water, the competitive nature of the solvent increases and the behaviour of the dyes changes dramatically. In fact, none of the squaraines shows a remarkable colour modulation in neat aqueous solution in the presence of metal ions except for $\mathbf{SNS_2O_2}$. This lack of signalling is observed even in acetonitrile–water mixtures with a relatively low content of around 3 wt% water. This behaviour originates from the strong solvation energy of the metal ions in the presence of water, which eventually disfavours metal–ligand interaction. Additionally, the behaviour showed by the $\mathbf{SNS_2O_2}$ receptor is highly selective and only the thiophilic Hg^{2+} cation is able to induce a colour

modulation from purple to colourless in water. The response of $\mathbf{SNS_2O_2}$ to several metal ions in buffered acetonitrile–water 20:80 (v/v) solutions (HEPES 0.08 M, pH 6.90, $c_{\mathbf{SNS_2O_2}} = 2\times10^{-6}$ mol L^{-1}) is shown in Figure 11, in which the absorbance of the dye at 640 nm in the presence of 100 equivalents of certain metal cations is displayed.[61] The system shows a remarkable behaviour with respect to the detection of Hg^{2+}, with a very low detection limit of 10^{-8} M and a complex stability constant of $\log K = 7.5$.

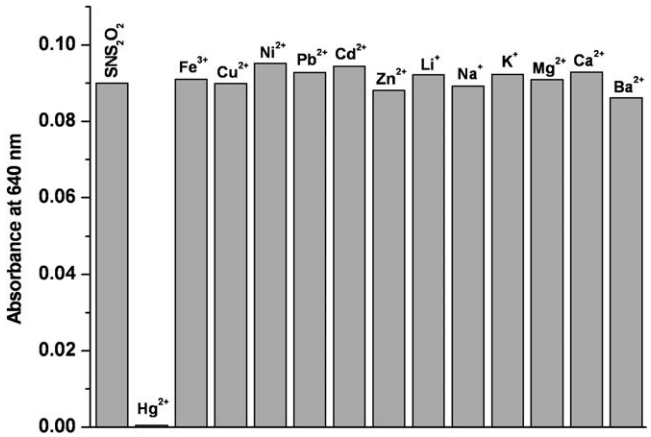

Figure 11. Absorbance at 640 nm for $\mathbf{SNS_2O_2}$ in the presence of 100 equivalents of metal cations in acetonitrile/water 20:80 (v/v) solutions, HEPES 0.08 M pH 6.90, $c_{\mathbf{SNS_2O_2}} = 2\times10^{-6}$ mol L^{-1}.

Conclusion

In conclusion, we have prepared and characterised a family of squaraine dyes and have studied their interaction and their photophysical properties. Squaraines such as the title compounds closely resemble cyanine dyes consisting of two substituted aniline moieties and a central four-membered squaric acid ring. In all cases, the squaraine derivatives show two distinct coordination sites at the anilino nitrogen and at the oxygen from the C_4O_2 central ring. Diverse colorimetric behaviour has been observed in the squaraine derivatives' interaction with protons and metal cations. In order to rationalise this colorimetric behaviour, we have performed semiempirical calculations and determined the stability constants of the complexes. Thus, the visible band of the squaraines at around 640 nm is blue-shifted when coordination at the anilino nitrogen atom occurs, whereas coordination to the C_2O_4 oxygen atoms results in the development of red-shifted bands. Addition of more than one equivalent of protons or metal ions could additionally lead to the formation of mixed N,O- or N,N-coordinated complexes, entailing the development of a broad band at 480 nm or bleaching, respectively. The presence of more complex species involving more than two coordinated metal ions has not been observed. Finally, the use of these coordinating dyes for the development of suitable chemical sensors and molecular-scale "logic gates" has been discussed. We believe that the present approach of approximating the signal expression of addressable squaraines will be useful in the future design of functional supramolecular ensembles based on this class of dyes.

Experimental Section

General remarks: All commercially available reagents were used without further purification. Air/water-sensitive reactions were performed in flame-dried glassware under argon. Acetonitrile and CH_2Cl_2 were dried with CaH_2 and distilled prior to use. 16-Phenyl-16-aza-1,4,7,10,13-pentaoxacyclooctadecane, 13-phenyl-13-aza-1,4,7,10-tetraoxacyclopentadecane, 10-phenyl-10-aza-1,4,7-trioxacyclododecane, *N*,*N*-di[ethyl-2-(2 methoxy)]aniline, 10-phenyl-10-aza-1,4-dioxa-7,13-dithiacyclopentadecane and 2-[(2-butylcarbamoiloxiethyl)phenylamine]ethyl ester were prepared following known procedures.[15,18,19,24,31,32]

Physical measurements and instrumentation: The NMR spectra were recorded with a Varian Gemini 300 spectrometer. Chemical shifts are reported in ppm downfield from the TMS signal. Spectra taken in $CDCl_3$ were referred to the residual $CHCl_3$.

General synthesis: **SNO$_3$**,[24] **SNO$_4$**,[24] **SNO$_5$**,[24] **SBu**,[31] **SJu**[32] and **SJuOH**[32] were prepared according to literature procedures. For **SAb**, **SCar** and **SNS$_2$O$_2$**, we employed the general synthetic procedure for squaraines.[62] *N*,*N*-Dibutyl aniline (3 mmols) and squaric acid (1.37 mmols) were dissolved in a 1:1 butanol/toluene mixture (25 mL). The crude reaction mixture was placed in a Dean–Stark apparatus, for the azeotropic removal of water, and heated under reflux for 5 h. On cooling the solution to room temperature green needles of the dyes precipitated. The solids were filtered off and washed with hexane to obtain the final products as green-blue solids.

Synthesis of bis(4-{bis[2-(2-methoxy-ethoxy)-ethyl]}aminophenyl)squaraine (SAb): Yield: 85.8 mg, 9.3 %; ^{1}H NMR: ($CDCl_3$): $\delta = 3.35$ (s, 12H; OCH_3), 3.48 (t, $J = 6.6$ Hz, 8H; CH_2CH_2NAr), 3.57 (t, $J = 7.0$ Hz, 8H; CH_2CH_2O), 3.66 (t, $J = 6.5$ Hz, 8H; CH_2CH_2O), 3.73 (t, $J = 6.8$ Hz, 8H; CH_2CH_2O), 6.79 (d, $J = 9.1$ Hz, 4H; Ar*H*), 8.33 ppm (d, $J = 9$ Hz, 4H;Ar*H*); ^{13}C NMR ($CDCl_3$): $\delta = 51.29$, 58.93, 68.23, 70.44, 71.72, 112.49, 119.88, 113.09, 153.75, 183.13, 188.56 ppm; mass IE high resolution calcd for $C_{36}H_{52}N_2O_{10}$: 673.3700; found: 673.3696.

Synthesis of bis(4-{bis[2-(butyl carbamic acid)-ethyl]}aminephenyl)squaraine (SCar): Yield: 174.1 mg, 15.2 %; ^{1}H NMR: $\delta = 0.85$ (t, $J = 6.6$ Hz, 12H; CH_2CH_3), 1.20–1.25 (m, 8H; $CH_2CH_2CH_3$), 1.35–1.43 (m, 8H; $CH_2CH_2CH_2$), 3.09 (q, $J = 5.9$ Hz, 8H; NHCH_2CH_2), 3.69 (t, $J = 6.6$ Hz, 8H; CH_2CH_2NAr), 4.23 (t, $J = 6.7$ Hz, 8H; CH_2CH_2O), 5.16 (m, 4H; CO*NH*CH$_2$), 6.79 (d, $J = 8.6$ Hz, 4H; Ar*H*), 8.31 ppm (d, $J = 8.4$ Hz, 4H; Ar*H*); ^{13}C NMR ($CDCl_3$): $\delta = 13.97$, 20.14, 32.16, 41.09, 50.91, 61.48, 113.17, 120.70, 133.73, 154.51, 156.42, 183.41, 190.55 ppm; mass FAB high resolution calcd for $C_{44}H_{64}N_6O_{10}$: 836.4721; found: 836.4684.

Synthesis of bis[4-(1,4-dioxa-7,13-dithia-10-aza-cyclopentadecane)phenyl]squaraine ($\mathbf{SNS_2O_2}$): Yield: 213.9 mg, 21.3 %; ^{1}H NMR ($CDCl_3$): $\delta = 2.77$ (t, $J = 7.4$ Hz, 8H; SCH_2), 2.93 (t, $J = 7.7$ Hz, 8H; SCH_2), 3.64 (s, 8H; OCH_2), 3.81 (m, 16H), 6.73 (d, $J = 9.1$ Hz, 4H; Ar*H*), 8.38 ppm (d, $J = 8.9$ Hz, 4H; Ar*H*); ^{13}C NMR ($CDCl_3$): $\delta = 189.94$, 183.43, 153.17, 133.81, 120.62, 112.89, 74.47, 70.94, 52.66, 32.13, 30.06 ppm; mass FAB high resolution calcd for $C_{36}H_{49}N_2O_6S_4$ MH$^+$: 733.247350; found: 733.247373.

Optical spectroscopy: UV/Vis spectra were recorded on a Bruins Instruments Omega 10 and a Perkin Elmer Lambda 35 spectrophotometer, steady-state fluorescence spectra on a Spectronics Instruments 8100 fluorometer (90° standard geometry, polarisers at 0° and 54.7° in excitation and emission). All photophysical measurements were carried out at 298 ± 1 K with dilute solutions with optical densities between 0.03 and 0.05 at the absorption maximum. Fluorescence quantum yields (Φ_f) were determined relative to rhodamine 101 in ethanol ($\Phi_f = 1.00 \pm 0.02$)[63] with uncertainties of ± 3 % (for $\Phi_f > 0.2$) and ± 6 % (for $0.2 > \Phi_f > 0.02$), respectively. All the fluorescence spectra were corrected as described in reference [64]. The Stokes shifts were calculated from the differences be-

tween the maxima of the absorption and emission bands after conversion to the energy scale, taking into account another correction step.[65] Fluorescence lifetimes (τ_f) were measured with a unique laser impulse fluorometer with picosecond time resolution described by us in an earlier publication[66] and modified according to a description in reference [67]. The fourth harmonic output of the signal of the OPA was used for excitation, the fluorescence was collected at right angles (polariser at 54.7°, monochromator with bandwidths of 4, 8, and 16 nm), and the decays were recorded by the single photon timing method (typical instrumental response functions of 25–30 ps full width at half maximum, experimental accuracy of ± 3 ps). The laser beam was attenuated using a double prism attenuator from LTB and typical excitation energies were in the nanowatt to microwatt range (average laser power). The fluorescence lifetime profiles were analysed with a PC using the software package Global Unlimited V2.2 (Laboratory for Fluorescence Dynamics, University of Illinois). The goodness of fit of the single decays as judged by reduced chi-squared (χ^2_R) and the autocorrelation function *C(j)* of the residuals was always below $\chi^2_R < 1.2$.

Theoretical studies: For the discussion in the photo-physical section, ground-state geometries were optimised using density functional theory (DFT) with Becke's three-parameter hybrid exchange functional[68] in conjunction with the Lee–Yang–Parr gradient-corrected correlation functional (B3LYP functional)[69] with the 6-31G basis set as implemented in Gaussian 03.[70] All the optimised structures were confirmed as energy minima by normal coordinate analysis. For the discussion of the protonation results, quantum chemical calculations at semi-empirical level (PM3, within restricted Hartree–Fock level) were carried out in vacuo with the aid of Hyperchem V6.03. The Polar Ribiere algorithm was used for the optimisation. The convergence limit and RMS gradient were set to 0.01 kcal m^{-1}.

Calculation of macroscopic binding constants: Spectrophotometric titrations were carried out in acetonitrile using a cuvette thermostated at 25 ± 0.1 °C. The titrant was added by means of a micropipette. The computer program HYPERQUAD 2000, version 2.1, was used to calculate the protonation and stability constants.[71] A typical titration experiment had about 4000 points (50 titration curves measured at 80 wavelengths) for each system. An excessive β limit of 0.33 and a maximum of 50 iterations were employed during the refining process.

Calculation of microscopic binding constants: For the calculation of the microscopic constants a general ligand (R) that can be protonated at two different sites to yield products A or B was considered. The coordination reactions and the microscopic constants k_a and k_b for coordination at site A or B, respectively, can be defined as given in Equations (3)–(5).

$$\begin{aligned}&\text{Reaction 1}: \ R + H \rightleftharpoons A\\ &\text{Reaction 2}: \ R + H \rightleftharpoons B\end{aligned} \tag{3}$$

$$k_a = \frac{[A]}{[R][H]} \tag{4}$$

$$k_b = \frac{[B]}{[R][H]} \tag{5}$$

For the overall reaction, the macroscopic constant K and an apparent molar extinction coefficient (ε_{ap}) can be calculated. For this macroscopic constant, the absorbance can be written as given in Equation (6) in which c_T the sum of the concentration of A (c_a) and B (c_b). We can also derive Equations (7) and (8)

$$A = c_T \varepsilon_{ap} \tag{6}$$

$$A = A_a + A_b = c_a \varepsilon_a + c_b \varepsilon_b \tag{7}$$

$$c_T \varepsilon a_p = c_a \varepsilon_a + c_b \varepsilon_b \tag{8}$$

For two different wavelengths (λ_1 and λ_2) Equations (9) and (10) follow:

$$\frac{c_T \varepsilon_{ap1}}{c_T \varepsilon_{ap2}} = \frac{c_a \varepsilon_{a1} + c_b \varepsilon_{b1}}{c_a \varepsilon_{a2} + c_b \varepsilon_{b2}} \tag{9}$$

$$\frac{\varepsilon_{ap1}}{\varepsilon_{ap2}} = \frac{(k_a/k_b) c_b \varepsilon_{a1} + c_b \varepsilon_{b1}}{(k_a/k_b) c_b \varepsilon_{a2} + c_b \varepsilon_{b2}} \tag{10}$$

This can be easily rearranged to give Equation (11):

$$\frac{k_a}{k_b} = \frac{\varepsilon_{b1} - (\varepsilon_{ap1}/\varepsilon_{ap2})\varepsilon_{b2}}{(\varepsilon_{ap1}/\varepsilon_{ap2})\varepsilon_{a2} - \varepsilon_{a1}} \tag{11}$$

The relation between the micro- and the macroscopic constants is given by Equation (12):

$$K = k_a + k_b \tag{12}$$

Working out K and replacing it in Equation (11) we are able to obtain Equation (13):

$$k_b = \frac{K}{[\{\varepsilon_{b1} - (\varepsilon_{ap1}/\varepsilon_{ap2})\varepsilon_{b2}\}/\{(\varepsilon_{ap1}/\varepsilon_{ap2})\varepsilon_{a2} - \varepsilon_{a1}\}] + 1} \tag{13}$$

In this equation, K, ε_{ap1} and ε_{ap2} data can be calculated by HYPERQUAD. On the contrary ε_{a1}, ε_{b1}, ε_{a2} and ε_{b2} were estimated from similar compounds displaying protonation only at one site.

Acknowledgements

We thank the Ministerio de Ciencia y Tecnología (project MAT2003-08568-C03 and CTQ2006-15456-C04-01/BQU) for support. J.V.R.-L. thanks the Generalitat Valenciana for a Postdoctoral Fellowship.

[1] A. Treibs, K. Jacob, *Angew. Chem.* **1965**, *77*, 680–681; *Angew. Chem. Int. Ed. Engl.* **1965**, *4*, 694.
[2] S. Sreejith, P. Carol, P. Chithra, A. Ajayaghosh, *J. Mater. Chem.* **2008**, *18*, 264–274; S. Yagi, H. Nakazumi in *Functional Dyes* (Ed.: S.-H. Kim), Elsevier, Amsterdam, **2006**, pp. 215–255.
[3] M. Tian, M. Furuki, I. Iwasa, Y. Sato, L. S. Pu, S. Tatsuura, *J. Phys. Chem. B* **2002**, *106*, 4370–4376; M. Emmelius, G. Pawlowski, H. W. Vollmann, *Angew. Chem.* **1989**, *101*, 1475–1502; *Angew. Chem. Int. Ed. Engl.* **1989**, *28*, 1445–1471; V. B. Jipson, C. R. Jones *J. Vac. Sci. Technol.* **1981**, *18*, 105–109.
[4] J. Wu, E. Huo, Z. Wu, Z. Lu, M. Xie, Q. Jiang, *e-Polym.* **2007**, no. 077; J. H. Yum, P. Walter, S. Huber, D. Rentsch, T. Geiger, F. Nüesch, F. De Angelis, M. Grätzel, M. K. Nazeeruddin, *J. Am. Chem. Soc.* **2007**, *129*, 10320–10321; A. Burke, L. Schmidt-Mende, S. Ito, M. Grätzel, *Chem. Commun.* **2007**, 234–236; S. Alex, U. Santhosh, S. Das, *J. Photochem. Photobiol. A* **2005**, *172*, 63–71; W. Zhao, Y. J. Hou, X. S. Wang, B. W. Zhang, Y. Cao, R. Yang, W. B. Wang, X. R. Xiao, *Sol. Energy Mater. Sol. Cells* **1999**, *58*, 173–183; A. P. Piechowski, G. R. Bird, D. L. Morel, E. L. Stogryn, *J. Phys. Chem.* **1984**, *88*, 934–950; V. Y. Merritt, H. J. Hovel, *Appl. Phys. Lett.* **1976**, *29*, 414–415.
[5] S. H. Hwang, N. K. Kim, K. N. Koh, S. H. Kim, *Dyes Pigm.* **1998**, *39*, 359–369; K. Y. Law, *J. Imaging Sci.* **1987**, *31*, 83–93; A. C. Tam, *Appl. Phys. Lett.* **1980**, *37*, 978–981.
[6] A. Ajayaghosh, *Chem. Soc. Rev.* **2003**, *32*, 181–191; L. Beverina, M. Crippa, P. Salice, R. Ruffo, C. Ferrante, I. Fortunati, R. Signorini, C. M. Mari, R. Bozio, A. Facchetti, G. A. Pagani, *Chem. Mater.* **2008**, *20*, 3242–3244; G. J. Ashwell, J. Ewington, K. Moczko, *J. Mater. Chem.* **2005**, *15*, 1154–1159; G. J. Ashwell, G. Jefferies, D. G. Hamilton, D. E. Lynch, M. P. S. Roberts, G. S. Bahra, C. R. Brown, *Nature* **1995**, *375*, 385–388; C. T. Chen, S. R. Marder, L. T. Cheng, *J. Am. Chem. Soc.* **1994**, *116*, 3117–3118; C. T. Chen, S. R. Marder, L. T. Cheng, *J. Chem. Soc. Chem. Commun.* **1994**, 259–260.
[7] R. Bonnett, *Chemical Aspects of Photodynamic Therapy*, Gordon and Breach, Amsterdam, **2000**, Chapter. 11; L. Beverina, M. Crippa, M. Landenna, R. Ruffo, P. Salice, F. Silvestri, S. Versari, A. Villa, L. Ciaffoni, E. Collini, C. Ferrante, S. Bradamante, C. M. Mari, R.

Bozio, C. A. Pagani, *J. Am. Chem. Soc.* **2008**, *130*, 1894–1902; L. Beverina, A. Abbotto, M. Landenna, M. Cerminara, R. Tubino, F. Meinardi, S. Bradamante, G. A. Pagani, *Org. Lett.* **2005**, *7*, 4257–4260; R. F. Santos, L. V. Reis, P. Almeida, A. S. Oliveira, L. F. Vieira Ferreira, *J. Photochem. Photobiol. A* **2003**, *160*, 159–161; D. Ramaiah, A. Joy, N. Chandrasekhar, N. V. Eldho, S. Das, M. V. George, *Photochem. Photobiol.* **1997**, *65*, 783–790.

[8] V. S. Jisha, K. T. Arun, M. Hariharan, D. Ramaiah, *J. Am. Chem. Soc.* **2006**, *128*, 6024–6025; C. Sun, J. Yang, L. Li, X. Wu, Y. Liu, S. Liu, *J. Chromatogr. B* **2004**, *803*, 173–190; B. Oswald, L. Patsenker, J. Duschl, H. Szmacinski, O. S. Wolfbeis, E. Terpetschnig, *Bioconjugate Chem.* **1999**, *10*, 925–931; E. Terpetschnig, H. Szmacinski, J. R. Lakowicz, *Anal. Chim. Acta* **1993**, *282*, 633–641; Smith and coworkers have published a series of studies on the performance of squaraine-rotaxane dyes as biochemical labels; see for example, J. J. Gassensmith, E. Arunkumar, L. Barr, J. M. Baumes, K. M. DiVittorio, J. R. Johnson, B. C. Noll, B. D. Smith, *J. Am. Chem. Soc.* **2007**, *129*, 15054–15059.

[9] A. Ajayaghosh, *Acc. Chem. Res.* **2005**, *38*, 449–459.

[10] P. T. Snee, R. C. Somers, G. Nair, J. P. Zimmer, M. G. Bawendi, D. G. Nocera, *J. Am. Chem. Soc.* **2006**, *128*, 13320–13321; Y. G. Isgor, E. U. Akkaya, *Tetrahedron Lett.* **1997**, *38*, 7417–7420.

[11] E. Arunkumar, A. Ajayaghosh, J. Daub, *J. Am. Chem. Soc.* **2005**, *127*, 3156–3164; M. A. Balbo Block, S. Hecht, *Macromolecules* **2004**, *37*, 4761–4769; E. Arunkumar, P. Chithra, A. Ajayaghosh, *J. Am. Chem. Soc.* **2004**, *126*, 6590–6598; U. Oguz, E. U. Akkaya, *Tetrahedron Lett.* **1998**, *39*, 5857–5860; C. R. Chenthamarakshan, A. Ajayaghosh, *Tetrahedron Lett.* **1998**, *39*, 1795–1798; E. U. Akkaya, S. Turkyilmaz, *Tetrahedron Lett.* **1997**, *38*, 4513–4516.

[12] J. Thomas, D. B. Sherman, T. J. Amiss, S. A. Andaluz, J. B. Pitner, *Bioconjugate Chem.* **2007**, *18*, 1841–1846; Y. Suzuki, K. Yokoyama, *Angew. Chem.* **2007**, *119*, 4175–4177; *Angew. Chem. Int. Ed.* **2007**, *46*, 4097–4099; B. Kukrer, E. U. Akkaya, *Tetrahedron Lett.* **1999**, *40*, 9125–9128.

[13] A. Ajayaghosh, P. Chithra, R. Varghese, K. P. Divya, *Chem. Commun.* **2008**, 969–971; K. Jyothish, M. Hariharan, D. Ramaiah, *Chem. Eur. J.* **2007**, *13*, 5944–5951; S.-Y. Hsueh, C.-C. Lai, Y.-H. Liu, S.-M. Peng, S.-H. Chiu, *Angew. Chem.* **2007**, *119*, 2059–2063; *Angew. Chem. Int. Ed.* **2007**, *46*, 2013–2017; A. Ajayaghosh, P. Chithra, R. Varghese, *Angew. Chem.* **2007**, *119*, 234–237; *Angew. Chem. Int. Ed.* **2007**, *46*, 230–233; R. S. Stoll, N. Severin, J. P. Rabe, S. Hecht, *Adv. Mater.* **2006**, *18*, 1271–1275.

[14] S. Das, K. G. Thomas, M. V. George in *Organic Photochemistry* (Eds.: V. Ramamurthy, K. S. Schanze), CRC, Boca Raton, FL (USA), pp. 467–517; K.-Y. Law in *Organic Photochemistry* (Eds.: V. Ramamurthy, K. S. Schanze), CRC, Boca Raton, FL (USA), pp. 519–584.

[15] J. V. Ros-Lis, R. Martínez-Máñez, K. Rurack, F. Sancenón, J. Soto, M. Spieles, *Inorg. Chem.* **2004**, *43*, 5183–5185.

[16] J. V. Ros-Lis, M. D. Marcos, R. Martínez-Máñez, K. Rurack, J. Soto, *Angew. Chem.* **2005**, *117*, 4479–4482; *Angew. Chem. Int. Ed.* **2005**, *44*, 4405–4407.

[17] D. Jiménez, R. Martínez-Máñez, F. Sancenón, J. V. Ros-Lis, A. Benito, J. Soto, *J. Am. Chem. Soc.* **2003**, *125*, 9000–9001; J. V. Ros-Lis, R. Martinéz-Máñez, J. Soto, *Chem. Commun.* **2002**, 2248–2249.

[18] J. V. Ros-Lis, B. García, D. Jiménez, R. Martínez-Máñez, F. Sancenón, J. Soto, F. Gonzalvo, M. C. Valldecabres, *J. Am. Chem. Soc.* **2004**, *126*, 4064–4065.

[19] J. V. Ros-Lis, R. Martínez-Máñez, J. Soto, *Org. Lett.* **2005**, *7*, 2337–2339.

[20] T. Gunnlaugsson, M. Glynn, G. M. Tocci, P. E. Kruger, F. M. Pfeffer, *Coord. Chem. Rev.* **2006**, *250*, 3094–3117; "Fluorescent Sensors": Guest Editor Issue, *J. Mater. Chem.* **2005**, *15 (27–28)*; R. Martínez-Máñez, F. Sancenon, *Chem. Rev.* **2003**, *103*, 4419–4476; A. P. de Silva, H. Q. N. Gunaratne, T. Gunnlaugsson, A. J. M. Huxley, C. P. McCoy, J. T. Rademacher, T. E. Rice, *Chem. Rev.* **1997**, *97*, 1515–1566.

[21] K. Y. Law, *J. Phys. Chem.* **1989**, *93*, 5925–5930.

[22] C. E. Silva, R. Diniz, B. L. Rodrigues, L. F. C. de Oliveira, *J. Mol. Struct.* **2007**, *831*, 187–194; C. W. Dirk, W. C. Herndon, F. Cervantes-Lee, H. Selnau, S. Martínez, P. Kalamegham, A. Tan, G. Campos, M. Velez, J. Zyss, I. Ledoux, L. T. Cheng, *J. Am. Chem. Soc.* **1995**, *117*, 2214–2225.

[23] R. W. Bigelow, H. J. Freund, *Chem. Phys.* **1986**, *107*, 159–174.

[24] S. Das, K. G. Thomas, K. J. Thomas, P. V. Kamat, M. V. George, *J. Phys. Chem.* **1994**, *98*, 9291–9296.

[25] C. Cornelissen-Gude, W. Rettig, R. Lapouyade, *J. Phys. Chem. A* **1997**, *101*, 9673–9677.

[26] K. Y. Law, *J. Phys. Chem.* **1987**, *91*, 5184–5193.

[27] D. C. Magri, T. P. Vance, A. P. de Silva, *Inorg. Chim. Acta* **2007**, *360*, 751–764; A. P. de Silva, Y. Leydet, C. Lincheneau, N. D. McClenaghan, *J. Phys. Condens. Matter* **2006**, *18*, S1847-S1872.

[28] G. Dilek, E. U. Akkaya, *Tetrahedron Lett.* **2000**, *41*, 3721–3724.

[29] V. Amendola, D. Esteban-Gomez, L. Fabbrizzi, M. Licchelli, E. Monzani, F. Sancenon, *Inorg. Chem.* **2005**, *44*, 8690–8698; B. D. Smith, J. M. Mahoney in *Encyclopedia of Supramolecular Chemistry* (Eds.: J. L. Atwood, J. L. Steed), Marcel Dekker, New York, **2004**, pp. 1291–1294; L. Kovbasyuk, R. Krämer, *Chem. Rev.* **2004**, *104*, 3161–3188; A. P. de Silva, G. D. McClean, S. Pagliari, *Chem. Commun.* **2003**, 2010–2011; H. Miyaji, S. R. Collinson, I. Prokes, J. H. R. Tucker, *Chem. Commun.* **2003**, 64–65.

[30] S. Yagi, Y. Hyodo, M. Hirose, H. Nakazumi, Y. Sakurai, A. Ajayaghosh, *Org. Lett.* **2007**, *9*, 1999–2002.

[31] K. Y. Law, F. C. Bailey, L. J. Bluett, *Can. J. Chem.* **1986**, *64*, 1607–1619.

[32] P. M. Kazmaier, G. K. Hammer, R. A. Burt, *Can. J. Chem.* **1990**, *68*, 530–536.

[33] K. Y. Law, *Trends Phys. Chem.* **1994**, *4*, 91–99.

[34] J. V. Caspar, T. J. Meyer, *J. Phys. Chem.* **1983**, *87*, 952–957; M. Bixon, J. Jortner, *J. Chem. Phys* **1968**, *48*, 715–726; W. Siebrand, *J. Chem. Phys.* **1967**, *46*, 440–447.

[35] J. F. Létard, R. Lapouyade, W. Rettig, *J. Am. Chem. Soc.* **1993**, *115*, 2441–2447; K. Rechthaler, G. Köhler, *Chem. Phys.* **1994**, *189*, 99–116; S. L. Wang, T. I. Ho, *Chem. Phys. Lett.* **1997**, *268*, 434–438.

[36] Note that the term "D–A(–D) dye" is used with a different connotation in the research communities on chromo/fluorogenic probes and on nonlinear optics. The first community almost exclusively refers to D–A(–D) dyes when such compounds show the typical features of ICT chromophores (considerably broad bands, strong solvatochromism).[35] The second community generally speaks of D–A(–D) or more often of D–π-A(–π-D) dyes, when molecules such as **M3** or **M5** are meant. Here, recently, a more detailed classification into class I D–π-A(–π-D) dyes (e.g., **M5**) and class II D–π-A(–π-D) dyes (e.g., **M3**) was proposed, cf. F. Terenziani, A. Painelli, C. Katan, M. Charlot, M. Blanchard-Desce, *J. Am. Chem. Soc.* **2006**, *128*, 15742–15755.

[37] B. Valeur, I. Leray, *Coord. Chem. Rev.* **2000**, *205*, 3–40; A. P. de Silva, H. Q. N. Gunaratne, T. Gunnlaugsson, A. J. M. Huxley, C. P. McCoy, J. T. Rademacher, T. E. Rice, *Chem. Rev.* **1997**, *97*, 1515–1566. ICT dyes are frequently also referred to as PCT (photoinduced charge transfer) dyes.

[38] S. Dähne, D. Leupold, *Angew. Chem.* **1966**, *78*, 1029–1039; *Angew. Chem. Int. Ed. Engl.* **1966**, *5*, 984–993; S. Dähne, *Science* **1978**, *199*, 1163–1167.

[39] W. Rettig, B. Strehmel, W. Majenz, *Chem. Phys.* **1993**, *173*, 525–537.

[40] W. Rettig, K. Rurack, M. Sczepan, in *New Trends in Fluorescence Spectroscopy* (Eds.: B. Valeur, J.-C. Brochon), Springer, Berlin, **2001**, pp. 125–155.

[41] J. Bendig, U. Schedler, T. Harder, P. Wessig, J. Lobedank, W. Grahn, *J. Photochem. Photobiol. A* **1995**, *91*, 53–57.

[42] A. Mishra, G. B. Behera, M. M. G. Krishna, N. Periasamy, *J. Lumin.* **2001**, *92*, 175–188.

[43] C. Gude, W. Rettig, *J. Phys. Chem. A* **2000**, *104*, 8050–8057.

[44] M. V. Barnabas, A. Liu, A. D. Trifunac, V. V. Krongauz, C. T. Chang, *J. Phys. Chem.* **1992**, *96*, 212–217.

[45] B. Strehmel, A. M. Sarker, H. Detert, *ChemPhysChem* **2003**, *4*, 249–259.

[46] P. V. Kamat, S. Das, K. G. Thomas, M. V. George, *J. Phys. Chem.* **1992**, *96*, 195–199.
[47] M. Vogel, W. Rettig, R. Sens, K. H. Drexhage, *Chem. Phys. Lett.* **1988**, *147*, 452–460.
[48] K. Y. Law, *J. Phys. Chem.* **1995**, *99*, 9818–9824.
[49] Substitution of one of the end groups does not only change the electronic nature of that group, but also converts a symmetric chromophore into an asymmetric one. From the literature on polymethine dyes, such effects are known to lead mostly to blue-shifted spectra, see, for example, A. D. Kachkovskii, *Russ. Chem. Rev.* **1997**, *66*, 647–664.
[50] B. García-Acosta, R. Martínez-Máñez, F. Sancenón, J. Soto, K. Rurack, M. Spieles, E. García-Breijo, L. Gil, *Inorg. Chem.* **2007**, *46*, 3123–3135.
[51] J. L. Bricks, J. L. Slominskii, M. A. Kudinova, A. I. Tolmachev, K. Rurack, U. Resch-Genger, W. Rettig, *J. Photochem. Photobiol. A* **2000**, *132*, 193–208.
[52] S. Das, P. V. Kamat, B. De la Barre, K. G. Thomas, A. Ajayaghosh, M. V. George, *J. Phys Chem.* **1992**, *96*, 10327–10330.
[53] M. L. Dekhtyar, W. Rettig, *J. Photochem. Photobiol. A* **1999**, *125*, 57–62; V. Bonaèiæ-Koutecký, K. Schöffel, J. Michl, *Theor. Chim. Acta* **1987**, *72*, 459–474.
[54] J. V. Ros-Lis, R. Martínez-Máñez, A. Benito, J. Soto, *Polyhedron* **2006**, *25*, 1585–1591; R. M. Izatt, K. Pawlak, J. S. Bradshaw, R. L. Bruening, *Chem. Rev.* **1991**, *91*, 1721–2085.
[55] H. Mrozek, H. Nikol, A. Vogler, F. Vögtle, *J. Photochem. Photobiol. A* **1994**, *84*, 227–231.
[56] A. B. Descalzo, R. Martínez-Máñez, R. Radeglia, K. Rurack, J. Soto. *J. Am. Chem. Soc.* **2003**, *125*, 3418–3419.
[57] A. B. Descalzo, R. Martínez-Máñez, F. Sancenón, K. Hoffmann, K. Rurack, *Angew. Chem.* **2006**, *118*, 6068–6093; *Angew. Chem. Int. Ed.* **2006**, *45*, 5924–5948; R. Martínez-Máñez, F. Sancenón, *Coord. Chem. Rev.* **2006**, *250*, 3081–3093. R. Martínez-Máñez, F. Sancenón, *J. Fluoresc.* **2005**, *15*, 267–285; S. L. Wiskur, H. Aït-Haddou, J. J. Lavigne, E. V. Anslyn, *Acc. Chem. Res.* **2001**, *34*, 963–972.
[58] V. Balzani, A. Credi, M. Venturi, *ChemPhysChem* **2003**, *4*, 49–59; F. M. Raymo, *Adv. Mater.* **2002**, *14*, 401–414.
[59] Although most of the reported logic gates operate with two different inputs (e.g., two metal ions) the use of different concentrations of a single metal ion (for instance, Hg^{2+} in this case) can also give logic truth tables when using squaraine derivatives, such as those we report here containing different binding sites and different colours depending on the number and position of the coordinated metal ions. We would like to point out that in these systems the A = 1/B = 0 and the A = 0/B = 1 cases are not intrinsically identical as we can imagine a system in which two different injectors can feed in an input (a Hg^{2+} solution of a certain concentration) to a vessel containing the squaraine **SNS_2O_2**. Such a disposition will develop a logic truth table such as that shown in Table 10.
[60] K. Rurack, C. Trieflinger, A. Koval'chuck, J. Daub, *Chem. Eur. J.* **2007**, *13*, 8998–9003; J. Matsui, T. Sodeyama, K. Tamaki, N. Sugimoto, *Chem. Commun.* **2006**, 3217–3219; A. Coskun, E. Deniz, E. U. Akkaya, *Org. Lett.* **2005**, *7*, 5187–5189; D. Jiménez, R. Martínez-Máñez, F. Sancenón, J. V. Ros-Lis, J. Soto, A. Benito, E. García-Breijo. *Eur. J. Inorg. Chem.* **2005**, 2393–2403; D. Jiménez, R. Martínez-Máñez, F. Sancenón, J. Soto, *Tetrahedron Lett.* **2004**, *45*, 1257–1259; K. Rurack, A. Koval'chuck, J. L. Bricks, J. L. Slominskii, *J. Am. Chem. Soc.* **2001**, *123*, 6205–6206.
[61] In acetonitrile/water 20:80 v/v, **SNS_2O_2** forms H-aggregates, the presence of which can be controlled by the choice of the acetonitrile:water ratio. For a more detailed description of the system, see reference [15].
[62] H. E. Sprenger, W. Ziegenbein, *Angew. Chem.* **1968**, *80*, 541–546; *Angew. Chem. Int. Ed. Engl.* **1968**, *7*, 530–535.
[63] D. F. Eaton, *Pure Appl. Chem.* **1988**, *60*, 1107–1114.
[64] U. Resch-Genger, D. Pfeifer, C. Monte, W. Pilz, A. Hoffmann, M. Spieles, K. Rurack, J. Hollandt, D. Taubert, B. Schönenberger, P. Nording, *J. Fluoresc.* **2005**, *15*, 315–336.
[65] J. R. Lakowicz, *Principles of Fluorescence Spectroscopy*, Plenum, New York, 2nd ed., **1999**, p. 52.
[66] U. Resch, K. Rurack, *Proc. SPIE-Int. Soc. Opt. Eng.* **1997**, *3105*, 96–103.
[67] Z. Shen, H. Röhr, K. Rurack, H. Uno, M. Spieles, B. Schulz, G. Reck, N. Ono, *Chem. Eur. J.* **2004**, *10*, 4853–4871.
[68] A. D. Becke, *J. Chem. Phys.* **1993**, *98*, 5648–5652.
[69] C. Lee, W. Yang, R. G. Parr, *Phys. Rev. B* **1988**, *37*, 785–789.
[70] Gaussian 03 (Revision D.01), M. J. Frisch, G. W. Trucks, H. B. Schlegel, G. E. Scuseria, M. A. Robb, J. R. Cheeseman, J. A. Montgomery Jr., T. Vreven, K. N. Kudin, J. C. Burant, J. M. Millam, S. S. Iyengar, J. Tomasi, V. Barone, B. Mennucci, M. Cossi, G. Scalmani, N. Rega, G. A. Petersson, H. Nakatsuji, M. Hada, M. Ehara, K. Toyota, R. Fukuda, J. Hasegawa, M. Ishida, T. Nakajima, Y. Honda, O. Kitao, H. Nakai, M. Klene, X. Li, J. E. Knox, H. P. Hratchian, J. B. Cross, C. Adamo, J. Jaramillo, R. Gomperts, R. E. Stratmann, O. Yazyev, A. J. Austin, R. Cammi, C. Pomelli, J. W. Ochterski, P. Y. Ayala, K. Morokuma, G. A. Voth, P. Salvador, J. J. Dannenberg, V. G. Zakrzewski, S. Dapprich, A. D. Daniels, M. C. Strain, O. Farkas, D. K. Malick, A. D. Rabuck, K. Raghavachari, J. B. Foresman, J. V. Ortiz, Q. Cui, A. G. Baboul, S. Clifford, J. Cioslowski, B. B. Stefanov, G. Liu, A. Liashenko, P. Piskorz, I. Komaromi, R. L. Martin, D. J. Fox, T. Keith, M. A. Al-Laham, C. Y. Peng, A. Nanayakkara, M. Challacombe, P. M. W. Gill, B. Johnson, W. Chen, M. W. Wong, C. Gonzalez, J. A. Pople, Gaussian, Inc., Pittsburgh, PA, **2004**.
[71] P. Gans, A. Sabatinni, A. Vacca, *Talanta*, **1996**, *43*, 1739–1753.
[72] F. Meyers, C.-T. Chen, S. R. Marder, J.-L. Brédas, *Chem. Eur. J.* **1997**, *3*, 530–537.
[73] M. C. Basheer, U. Santhosh, S. Alex, K. G. Thomas, C. H. Suresh, S. Das, *Tetrahedron* **2007**, *63*, 1617–1623.
[74] Note that for all the compounds analysed here, the HOMO–LUMO contributes >65% to the lowest-energy allowed transition as derived from ZINDO calculations performed on the optimised B3LYP geometries (ZINDO/S with single configuration interaction (SCI) involving singly excited configurations generated from all occupied and unoccupied d-type molecular orbitals).

Received: February 18, 2008
Revised: June 24, 2008
Published online: September 11, 2008

